COMMENT

ON THE REFRACTIVE INDEX CORRECTION IN LUMINESCENCE SPECTROSCOPY

M.D. EDIGER, R.S. MOOG, S.G. BOXER and M.D. FAYER
Chemistry Department, Stanford University, Stanford, California 94305, USA

Received 14 December 1982; in final form 16 February 1982

The derivation of the refractive index (n) correction in luminescence spectroscopy is extended to cases with wide excitation beams. The accepted "$1/n^2$ correction" is found to be valid for a large number of experimental arrangements in contrast to the analysis of a recent paper.

1. Introduction

For more than thirty years, investigators have recognized that luminescence measurements made with certain experimental geometries require corrections for the refractive index of the solution [1,2]. These corrections are necessary when the ratio of luminescence from two solutions is required, as in relative quantum yield measurements [3]. In many cases, the magnitude of these corrections is not small. The widely utilized "$1/n^2$ correction", for example, amounts to more than 25% when comparing solutions in benzene (n = 1.50) and water (n = 1.33). Recently there has been some discussion regarding the appropriateness of this correction [4]. In this paper, we extend the analysis of the index of refraction correction, and show that a correction factor of $1/n^2$ is appropriate for common experimental geometries.

2. Previous approaches

Many experimentalists have used the correction derived by Hermans and Levinson [1] for the right angle geometry (i.e. collection optics normal to a cuvette surface and perpendicular to the excitation beam, as in fig. 1). The expression they derived for J, the collected light intensity (light passing through a monochromator slit),

$$J = Is_1s_2h/n^2b^2 , \qquad (1)$$

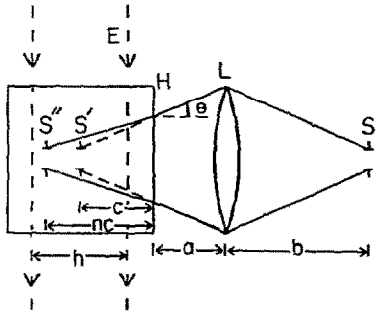

Fig. 1 Experimental geometry. E: excitation beam of width h; H: cuvette; L: lens of area s_1 and diameter d; S: slit of area s_2; S'. position of slit image in air (n = 1), S'': position of slit image in a solution of refractive index n, c. distance from S' to cuvette front, a, b. distances as shown.

is valid when the collection optics sample a uniformly luminescent area of the cuvette and the solid angle of light collected is small (i.e. paraxial conditions, $\sin\theta \approx \theta$). In eq. (1), I is proportional to the emission intensity in the direction of the collection optics and all other quantities are defined in fig. 1.

This derivation is strictly valid only when the excitation beam contains the slit image and in the limit that the width of the excitation beam, h, is small. Hermans and Levinson [1] only consider light coming from the plane defined by the image of the slit in the solution (slit image plane, S''), and use the solid angle subtended by the lens to calculate the fraction of this light passing through the slit (see eqs. (7) and (8) in

ref. [1]. They apply the results of this analysis to points in front and behind the slit image plane. However, not all of the solid angle of light collected by the lens from these points necessarily passes through the slit, as will become clear in section 3. Despite the limitations of the earlier derivation, a more detailed analysis (section 3) will show that for many typical geometries involving excitation beams of reasonable width, eq. (1) is in fact valid.

A recent paper by Busselle et al. [4] concludes that the n^2 factor is not required in eq. (1). Their derivation is essentially the same as the one outlined above except that the authors state that the slit image area in a solution of refractive index n is $m^2 s_2 n^2$ (in our notation), where m is the magnification of the optical system. This is incorrect. The correct area is $m^2 s_2$, as can be seen by examining fig. 2.

In fig. 2a, the image of point A is formed where the two light rays shown intersect at B [5]. All other rays starting from A and passing through the lens also intersect at B.

In fig. 2b, we consider the case in which the image of A is formed inside a solution of refractive index n. Since the ray through C is not refracted at the solution–air interface, the image of point A is formed at the same distance from the optical axis as in fig. 2a. Thus, in this example, the image of the arrow will be the same size in the two figures, although located at different positions. For any optical system in which an image is formed, this is true as long as the optical axis is normal to the interface of the two media. (This is the case treated by Busselle et al. and this paper.) If the arrow is replaced by a two-dimensional object (e.g. a slit), the image size will also be *independent* of the refractive index as above.

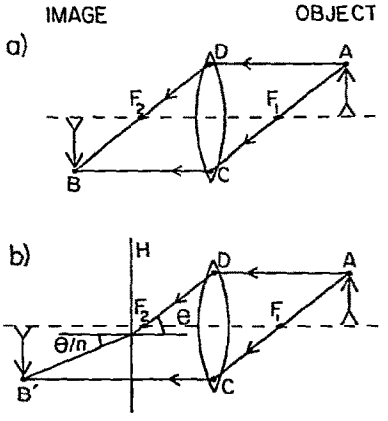

Fig. 2. Image size as a function of n. F_1, F_2: focal points; H: cuvette wall. The dotted line is the optical axis.

When the analysis of Busselle et al. is modified using the correct expression, $m^2 s_2$, as the slit image area, their equation for the relative luminescence intensities of two solutions of different refractive index becomes

$$J_1/J_2 = I_1 n_2^2 / I_2 n_1^2 . \quad (2)$$

This result is consistent with eq. (1).

The two derivations noted thus far are incomplete since they apply only in the slit image plane. For an excitation beam of a width typically used in an experiment, the applicability of these results is not obvious. Furthermore, since the slit image position changes with n, a very thin beam will fulfill the conditions of the derivation only if its position in the cuvette is adjusted as a function of the refractive index of the solution.

In order to have confidence in experimental results obtained under typical laboratory conditions, a more complete theoretical analysis is needed. We will use a numerical calculation based on geometric optics that considers not only emission from points in the slit image plane, but also from points a finite distance away from it. This necessitates a numerical integral over the entire volume illuminated within the cuvette.

3. Description of calculations

Using geometric optics, one can demonstrate that the collection system shown in fig. 1 is equivalent to that of fig. 3 for the purpose of calculating the light intensity passing through the slit. In fig. 3 the index of refraction is taken to be the same inside and outside the cuvette, and this change is compensated for by replacing θ with θ/n and a by na. This approach eliminates the need to explicitly include the effects of Snell's law in the analysis. We assume paraxial conditions. (The cuvette walls are taken to be thin for the case shown in fig. 3, although this is not necessary. The results presented will be correct for any reasonable wall thickness.) The slit and lens were chosen to be

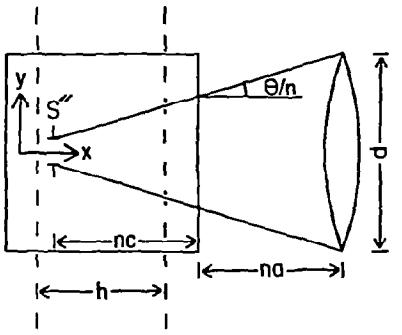

Fig. 3. Geometry of equivalent optical system. See text and previous figure captions for definitions of symbols.

circular to give the problem cylindrical symmetry. The precise shape of these elements does not affect the results presented. This was verified by also performing the calculation for the case of a rectangular slit and a circular lens (see section 4). The description that follows is given in terms of the simpler case with cylindrical symmetry.

We need to calculate J, the light intensity passing through the slit, for a given geometry (fixed a, c, d, h, n, and the slit image area in fig. 3). Due to the cylindrical symmetry of the problem, we work in a coordinate system in which x is the axis of symmetry and y is perpendicular to it. First, treat a point (x, y) in the illuminated region of the cuvette as an isotropic emitter and calculate F, the fraction of light from (x, y) passing through the slit. Second, weight F by the volume element, $2\pi y \Delta y \Delta x$, where Δx and Δy are the step sizes for the numerical integration. Finally, integrate over the appropriate volume (i.e. sum the weighted fractions to obtain J).

To carry out the above procedure, we need a method for calculating F. Not every photon passing through the lens contributes to J. In order for a photon to pass through the slit, it must go through the lens and either (i) come from S'', or (ii) be traveling with a trajectory such that its path is indistinguishable from that of a photon originating in S''. Therefore, only points within the labeled regions of fig. 4a can contribute to the integration. Of course, since only illuminated molecules can emit, the location and width of the excitation beam further limits the integration volume. At any (x, y), the fraction of light passing

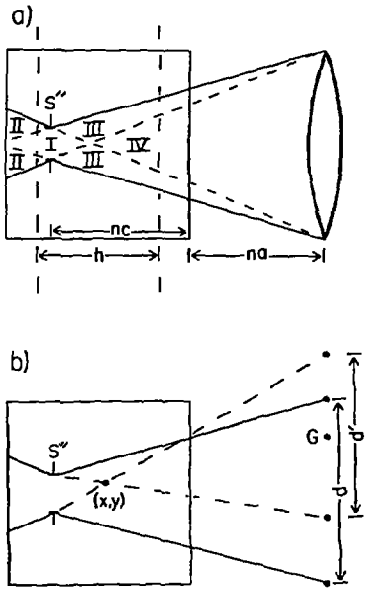

Fig. 4. (a) Different regions which can contribute to flux through the slit. (b) Projection of the slit image, S'', through (x, y) onto the plane of the lens. The intersection of this circle (diameter d', center at G) with the lens (diameter d) gives the area needed to determine the solid angle used in the calculation of the fraction of light entering the slit for any of the regions shown in (a). For (x, y) behind the slit image, the projection of S'' is found by drawing lines from (x, y) through the two edges of S'', and extending these lines to the plane which contains the lens. (Note that this figure applies to the case of cylindrical symmetry described in section 3.)

through the lens is $\Omega/4\pi$, where Ω is the solid angle subtended by the lens. Only in region I, however, does all this light pass through the slit. Thus in region I, $F = \Omega/4\pi$. In any other labeled region, part of the light passing through the lens will be refracted such that it does not pass through the slit. To find F, it is necessary to project S'' through (x, y) onto the plane which contains the lens (see fig. 4b). The area of intersection of this circle (the projection of S'') and the lens, divided by the square of the distance between (x, y) and the center of the intersection area, is the solid angle of light which contributes to flux through the slit. This solid angle divided by 4π is F for any region in fig. 4a. Outside the labeled regions, the area of intersection of the two circles, and hence F, is zero.

In addition to paraxial conditions, we have assumed that the chromophores in solution are randomly oriented and that the solution is uniformly luminescent over the volume defined by the width h and the areas sampled by the slit.

We should emphasize that this calculation was performed only for the simple collection optics shown in fig. 1. Other optical systems could be treated in an analogous manner. Furthermore, these calculations do not include the effects of reflective losses at the solution–cuvette interfaces. The magnitude of this effect (for both excitation and emission) is easily included in the analysis of experimental data, and will change the ratio of the intensities J_1/J_2 by less than 1% for a quartz cuvette and solution refractive indices between 1.33 and 1.5. Ignoring the *angular* dependence of the reflective loss introduces an error of less than 0.1% given paraxial conditions.

4. Results

Calculations were performed for geometries encompassing most common experimental arrangements of collection optics. For each geometry, light intensities for solutions of two different refractive indices ($n_1 = 1.33$, $n_2 = 1.5$) were calculated. The ratio of the intensities J_1/J_2 was compared to $(n_2/n_1)^2$. These quantities were identical to within 0.5% for all cases reported in table 1. Excluding cases where θ approached 10° (see fig. 1), these quantities were identical to within 0.2%. These results are valid for all $h \geqslant 1$ mm and all excitation beam locations possible in a 1 cm cuvette. They are independent of the magnification of the optical system. (Note that the slit *image* radius is used in table 1.) The position of the slit image was varied ±1 cm from the center of the cuvette (except for the first line of table 1, where ±0.5 cm was used). In addition to verifying that the $1/n^2$ correction is accurate within the limits described above, our calculations also show that the scaling for s_1, s_2 and h predicted by eq. (1) is approximately correct. Cases intermediate to those shown in table 1, or with a smaller difference between n_1 and n_2, also gave results consistent with those described above.

Table 1
Typical geometries examined

Lens–cuvette distance (cm)	Range of lens diameters (cm)[a]	Range of slit image diameters (mm)
4	0.6–1.3	0.04–4.0
12	1.0–4.0	0.04–4.0
20	1.0–6.6	0.04–4.0

a) The upper limits in this column define the maximum lens size allowable within the paraxial condition assumed in these calculations.

As noted in section 3, the case of a rectangular slit and circular lens was also treated. A range of slit heights (0.04–10 mm) and slit widths (0.04–3 mm) was considered for cases analogous to those in table 1. $(n_2/n_1)^2$ and the numerically calculated value for J_1/J_2 were identical within the limits specified above, except in a few instances (e.g. extremely narrow slits). For the latter cases, the larger deviation arose because the numerical integration was terminated before convergence to avoid excessive consumption of computer time. Even so, these two quantities were within 2.5%, and extrapolation of the calculated values of J_1/J_2 as a function of the step size indicated that further decreases in step size would result in convergence within the given limits.

In summary, we have corrected the treatment of Busselle et al. and extended the analysis of the refractive index correction to cases where the excitation beam is not thin. For the situations described in this section and in table 1, the $1/n^2$ caling predicted by Hermans and Levinson [1] is found to be correct. It should be emphasized that these results apply only in the paraxial limit for a solution which is uniformly luminescent over the volume sampled by the slit. As Busselle et al. have pointed out, the latter condition is often not met with respect to slit height. An additional correction (see section 3) due to reflective loss at the cuvette–solution interfaces should be included to complete the analysis of experimental data. Investigators utilizing experimental conditons similar to those described here should feel confident in applying the $1/n^2$ correction. The correction for systems of collection optics much different than those described here could be calculated using the procedure outlined in this paper.

Acknowledgement

We thank the National Science Foundation, DMR 79-20380 and PCM 79-26677, for supporting this work. SGB also acknowledges the Alfred P. Sloan Foundation and the Camille and Henry Dreyfus Foundation. MDE thanks the National Science Foundation for a Predoctoral Fellowship.

References

[1] J.J. Hermans and S. Levinson, J. Opt. Soc. Am. 41 (1951) 460.
[2] Th. Förster, Fluoreszenz Organischer Verbindungen (Vandenhoeck–Ruprecht, Gottingen, 1951).
[3] J.N. Demas and G.A. Crosby, J. Phys. Chem. 75 (1971) 991.
[4] F.J. Busselle, N.D. Haig and C. Lewis, Chem Phys Letters 72 (1980) 533.
[5] E. Hecht and A. Zajac, Optics (Addison-Wesley, Reading, 1974).